



**HAL**  
open science

## Influence of water ageing on the mechanical properties of flax/PLA non-woven composites

Delphin Pantaloni, Alessia Melelli, Darshil U. Shah, Christophe Baley, Alain Bourmaud

► **To cite this version:**

Delphin Pantaloni, Alessia Melelli, Darshil U. Shah, Christophe Baley, Alain Bourmaud. Influence of water ageing on the mechanical properties of flax/PLA non-woven composites. *Polymer Degradation and Stability*, 2022, 200, 10.1016/j.polymdegradstab.2022.109957 . hal-04585214

**HAL Id: hal-04585214**

**<https://hal.science/hal-04585214v1>**

Submitted on 22 Jul 2024

**HAL** is a multi-disciplinary open access archive for the deposit and dissemination of scientific research documents, whether they are published or not. The documents may come from teaching and research institutions in France or abroad, or from public or private research centers.

L'archive ouverte pluridisciplinaire **HAL**, est destinée au dépôt et à la diffusion de documents scientifiques de niveau recherche, publiés ou non, émanant des établissements d'enseignement et de recherche français ou étrangers, des laboratoires publics ou privés.



Distributed under a Creative Commons Attribution - NonCommercial 4.0 International License

1 **Influence of water ageing on the mechanical properties of flax/PLA non-woven composites**

2 Delphin Pantaloni<sup>a</sup>, Alessia Melelli<sup>a</sup>, Darshil. U. Shah<sup>b</sup>, Christophe Baley<sup>a</sup> and Alain Bourmaud<sup>a</sup>

3 a : Université de Bretagne-Sud, IRDL, CNRS UMR 6027, BP 92116, 56321 Lorient Cedex, France

4 b : Centre for Natural Material Innovation, Department of Architecture, University of

5 Cambridge, Cambridge CB2 1PX, United Kingdom

6 \* Corresponding author: [alain.bourmaud@univ-ubs.fr](mailto:alain.bourmaud@univ-ubs.fr) Tel.: +33-2-97-87-45-18

7 **Abstract**

8 Flax fibres are widely used in the automotive sector to reinforce polyolefins, such as for  
9 dashboard and interior door panels. A promising option is poly-(lactid) (PLA), as it leads to  
10 higher mechanical properties and offers an additional end-of-life scenario following recycling:  
11 industrial composting. However, like other composite systems such as flax/polyolefin, flax/PLA  
12 composites are also sensitive to water. Here, a non-woven flax/PLA composite is aged under  
13 several conditions (50% RH/75% RH/98% RH/Immersion) until saturation. After ageing, all  
14 samples are reconditioned at 50% RH, and their residual properties are assessed. The presence  
15 of a critical relative humidity between 75% and 98% is highlighted, above which, increases in  
16 moisture content irreversibly decrease the composite's mechanical properties. After ageing at  
17 98% RH and in immersion, tangent modulus was reduced by 23.0 and 33.8% and ultimate  
18 strength by 26.7 and 37.4%, respectively, compared to reference materials. This decrease is  
19 mainly due to microstructure evolution in the form of increasing porosity. This microstructure  
20 evolution is induced by the swelling of flax fibres, which generates high local stresses, above  
21 what PLA can withstand. As a result, micro-cracks appear in the matrix, responsible for  
22 reduction in mechanical properties.

23 **Keywords** : Biocomposites ; Flax fibres ; Non-woven ; Degradation ; Microstructure ; Moisture

## 24 **1 Introduction**

25 Thanks to their light weight [1] and their good mechanical properties [2], flax fibres can be  
26 drop-in alternatives to glass fibres as composite material reinforcements in the automotive  
27 area [3]. In addition, using thermoplastics as matrices reduces the composite's environmental  
28 impacts, especially thanks to recycling [4], which is a potential end-of-life solution for  
29 circularity. However, one of the bottlenecks for wider applications is the sorption behaviour of  
30 flax composites, especially when considering stringent validation standards of the automotive  
31 industry, which impose the test of materials across a large range of humidity and temperature  
32 conditions [5].

33 An elementary flax fibre, not embedded in a matrix, has a moisture content of 6% at 50%  
34 relative humidity (RH) and reaches 18% at 98% RH [6]. Flax sorption behaviour follows Park's  
35 model [7,8], divided into three sorption mechanisms, depending on the relative humidity. The  
36 first part follows Langmuir's sorption, where water molecules attach on specific sites of  
37 interactions. The second is described by Henry's sorption, where water uptake evolves linearly  
38 with the relative humidity, and the final stage occurring at high relative humidity is the  
39 clustering of water molecules in the remaining free spaces. Combining these three phenomena  
40 leads to a sigmoidal relation between the relative humidity and the moisture content in the  
41 flax fibres [6]. Interestingly, this phenomenon presents a hysteresis loop meaning that the  
42 water content of flax is not the same at a given relative humidity depending on if it is in the  
43 dynamic state of sorption or desorption [6]. Furthermore, this water uptake induces radial  
44 swelling of the flax fibre, correlating linearly with the hygro-expansion coefficient, measured to  
45 be  $1.14 \epsilon/\Delta m$  by Le Duigou et al. [9].

46 The moisture uptake in a composite is mainly due to flax fibres' water sorption behaviour and

47 the presence of a fibre/matrix interface [10], even for a hydrophilic matrix (PHBV) [11]. The  
48 sigmoidal sorption/desorption behaviour is also observed at the composite level [5]. For non-  
49 woven flax/PP composite (50wt%), Gager et al. [5] report a moisture content of 2.6% at 50%  
50 RH and 8% at 98% RH. The volume fraction of fibres impacts the moisture sorption of the  
51 composites [12]. However, the classical rule of mixture cannot predict the moisture uptake of  
52 the composites at high relative humidity. It appears coherent with experimental values at 75%  
53 RH but overestimates them at 98% RH [12]. This deviation at high relative humidity is  
54 explained by El Hachem et al. [12] by the containment effect of the matrix on the flax fibres,  
55 limiting their moisture uptake potential. Indeed, flax swelling is observed at the composite  
56 scale at a lower amplitude, as the matrix constrains fibre displacement [13].

57 This moisture uptake induces a decrease in stiffness and ultimate strength of the composite  
58 [5,10,14]. The origin of this decrease is still discussed in the literature [15–17], and several  
59 phenomena appear to be involved. It is reported for thermoset flax composites that cracks  
60 appear in the matrix [14,17], inducing debonding at the flax/matrix interface [14,15,17] and  
61 flax fibre damage [15,17,18]. All these phenomena are reported to be linked with the swelling  
62 of flax fibres inside the composite. However, there is no consensus because the phenomena  
63 observed varies depending on the ageing conditions, the experimental methods, and the flax  
64 composite mesostructure such as porosity, fibre volume fraction, fibre individualisation and  
65 fibre orientation. As an example, Chilali et al. [19] observed that the presence of sealed edges,  
66 inducing a preferential water diffusion direction, impacts the sorption kinetics and the ageing  
67 behaviour. Indeed, they suggest several damage mechanisms depending on the type of  
68 diffusion.

69 This paper focuses on the hygroscopic ageing of flax/PLA non-woven composite through its  
70 mesostructure and mechanical property evolution. Several hygroscopic conditions are

71 investigated (50% RH / 75% RH / 98% RH) as well as immersion ageing. The sorption kinetics  
72 are followed through weight monitoring, and the residual composite mechanical properties  
73 are measured. The mechanical properties of flax cell walls and matrix after ageing are also  
74 investigated at microscale thanks to AFM Peakforce measurements in mechanical mode (AFM-  
75 PF-QNM). Finally, the structure of the composite is examined through density measurement  
76 and SEM observation.

## 77 **2 Materials and methods**

### 78 2.1 Materials

#### 79 2.1.1 Raw materials

80 An industrial non-woven flax/PLA preform of 350 g/m<sup>2</sup> with a flax weight fraction of 40%, was  
81 manufactured on a needle-punching industrial line (Ecotechnilin, Yvetot, France). The non-  
82 woven has a preferred fibre direction. Indeed, the machine direction has slightly more  
83 oriented fibres in these industrial non-wovens [20]. The raw materials used are scutched flax  
84 tows and INGEO™ PLA fibres. Thanks to the needle-punching line, flax and PLA fibres are  
85 commingled together, leading to the non-woven preform.

#### 86 2.1.2 Composite manufacturing

87 Composite manufacturing is done through an optimised thermo-compression cycle of eight  
88 minutes using a hydraulic press LabTech Scientific 50T (Labtech, Samutprakarn, Thailand)  
89 press, set at 200°C. This processing cycle is presented in a previous study [21]. Eight plies of  
90 200x200 mm are stacked together and then dried at 40°C under vacuum for 24h. During the  
91 lay-up step, the specific orientation of the preforms is maintained. Therefore, thermo-  
92 compression leads to a composite with a preferential orientation of fibres, identical to the  
93 preform.

94 Next, dog-bone samples, according to the ISO 527-4 standard, are cut from the 2 mm thick

95 composite plates using a milling machine. The centre part of the dog bone has a width of 8  
 96 mm, a length of 45 mm and a thickness of 2 mm. The edges of the samples were not sealed to  
 97 be consistent with industrial applications. Thus, after cutting, flax fibres appear accessible in  
 98 the edges. Furthermore, the milling process damages the edges by initiating defects, which are  
 99 likely to influence the ageing response of the composite.

## 100 2.2 Methods

### 101 2.2.1 Ageing protocol

102 Once manufactured, samples are stored in a controlled humidity chamber at 50% RH. Once the  
 103 weight is stabilised, five samples are dried for 48h in an oven at 105°C and weighted. The initial  
 104 moisture content of samples, obtained through the mean of the five values, is  $2.6 \pm 0.1$  %. The  
 105 remaining samples are separated into five batches. One stays in the 50% RH chamber until  
 106 the end of the experiments and is called the 50\_RH\_ref batch. Others undergo humidity ageing  
 107 (also called vapour ageing) at 50%, 75% or 98% RH thanks to humidity chambers  
 108 (corresponding batches are labelled 50\_RH/ 75\_RH/ 98\_RH) or immersion ageing in distilled  
 109 water (corresponding batch is called Immersion). Ageing is conducted over a period of six  
 110 weeks. The humidity in the chambers is controlled thanks to saturated salt solutions. The salt  
 111 used and the exact relative humidity condition, controlled using testo 174H captors (Testo Inc.,  
 112 West Chester, USA), are presented in Table 1.

113

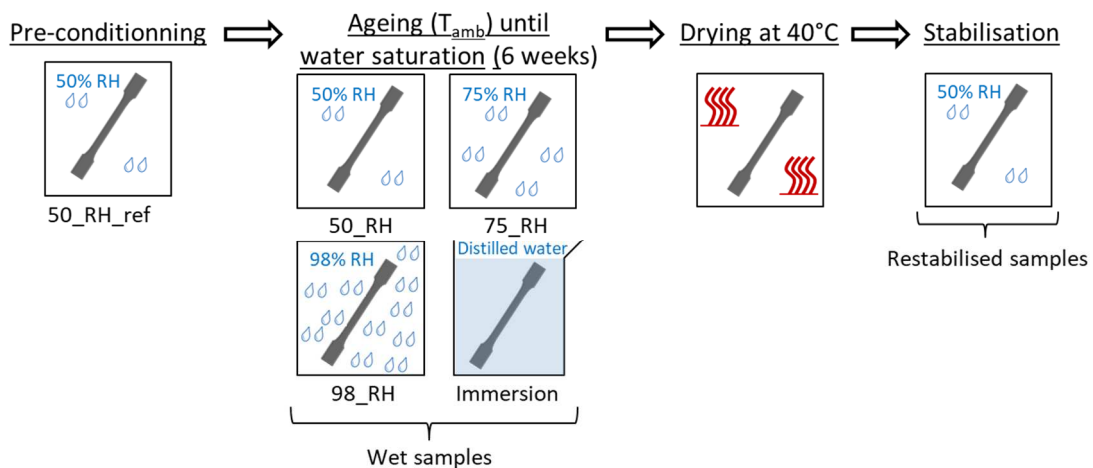
114 **Table 1.** Salt used for conditioning the chambers and the exact relative humidity condition  
 115 induced by them.

	Temp. [°C]	50% RH	75% RH	98% RH
Mean value [%]	$23.3 \pm 2.2$	$55.7 \pm 2.9$	$77.2 \pm 1.9$	$99.7 \pm 0.8$
Salt used	/	$\text{Mg}(\text{NO}_3)_2$	NaCl	$\text{K}_2\text{SO}_4$

116

117 Five samples of each batch are regularly weighted to obtain the weight evolution. After six  
118 weeks, once their weight stabilises, the 50\_RH / 75\_RH / 98\_RH / Immersion samples are dried  
119 at 40°C until stabilisation. This drying step allows avoiding the hysteresis consideration of flax  
120 fibre sorption [6]. Finally, all samples are stabilised again at 50% RH. This ageing protocol is  
121 summarized in Figure 1. The difference between the 50\_RH\_ref and the 50\_RH batches  
122 remains in the drying and restabilisation step, which are not applied to the 50\_RH\_ref  
123 samples. All the ageing protocol is done at room temperature. In the following discussions,  
124 wet samples (or wet state) will refer to the samples in saturated state during ageing. The  
125 restabilised samples (or restabilised state) will refer to the samples that have undergone  
126 ageing, drying and restabilisation at 50% RH.

127



128

129 **Figure 1.** Schematic representation of the ageing protocol applied to a flax/PLA non-woven  
130 composite with a fibre volume fraction of 36%.

131

132 2.2.2 Water content

133 As described before, samples are regularly weighted using a Fisherbrand™ (Fisher Scientific  
134 SAS, Illkirch Cedex, France) scientific high precision scale having a precision of  $10^{-4}$  g. The  
135 sampling depends on the stage of composite sorption, being narrow at the beginning of the  
136 sorption phenomenon. The moisture content at a given time ( $M_c(t)$ ) is calculated from the  
137 weight evolution using equation (1).

$$M_c(t) = \frac{W(t) - W_{dry}}{W_{dry}} \quad (\text{Equ.1})$$

138 Where  $W(t)$  is the sample weight at time  $t$  and  $W_{dry}$  is its dry weight. The dry weight of each  
139 sample is calculated equal to 97.4% of the initial mass of the samples as the initial moisture  
140 content was measured to be 2.6%. It avoids the drying step for samples before ageing, as it  
141 impacts the materials [22].

142 The sorption kinetics of the samples during ageing is discussed using Fick's law [11], equation  
143 (2), where  $D_{diff}$  is the diffusion coefficient, and  $h$  is the sample thickness. The initial moisture  
144 content and the moisture content at saturation are  $M_{c,init}$  and  $M_{\infty}$ , respectively. They are  
145 extracted from the experimental data for each ageing condition.

$$M_c(t) = (M_{\infty} - M_{c,init}) \cdot \left( 1 - \frac{8}{\pi^2} \sum_{n=0}^{\infty} \frac{1}{(2n+1)^2} \cdot \exp \frac{-\pi^2 \cdot (2n+1)^2 \cdot D_{diff} \cdot t}{h^2} \right) + M_{c,init} \quad (\text{Equ.2})$$

146 The diffusion coefficient ( $D_{diff}$ ) is calculated for all experimental points in the linear part of  
147 the experimental curves ( $M_c(t) < 0.5M_{\infty}$ ) using equation (3). The mean diffusion coefficient is  
148 used to implement Fick's law, equation (2).

$$D_{diff} = \pi \cdot \frac{h^2}{16 \cdot t} \cdot \left( \frac{M_c(t) - M_{c,init}}{M_{\infty}} \right) \quad (\text{Equ.3})$$

149 2.2.3 Mechanical characterisation through tensile tests

150 A universal Instron (Instron, Norwood, Massachusetts, USA) tensile machine is used with a  
151 10kN load cell. The tensile test is based on the ISO 527-4 standard, using a cross-head speed of  
152 1 mm/min. The elongation of the samples is measured with an Instron extensometer having a  
153 gauge length of 25 mm. The stiffness is calculated between 0.02% and 0.1%. At least nine  
154 samples are tested, and the mean value is extracted. Standard deviations are used as errors.  
155 The tensile tests are only done on restabilised samples.

156 2.2.4 Density measurement

157 The density was obtained through a hydrostatic balance using ethanol as immersion liquid,  
158 leading to the density of the composites. Samples for density measurement are cut from the  
159 central part of the dog bone samples (2 x 8 x 45 mm) thank to a circular saw as it is the part  
160 loaded in the measurement of mechanical properties. This extraction is done on restabilised  
161 samples. Density results are given as mean values of at least five samples.

162 Thanks to the apparent density of the composite ( $\rho_c$ ), the volume fraction of porosity ( $V_p$ ) of  
163 each batch is estimated using equation (4). The weight fraction of fibres  $W_f$  are 40% here. The  
164 density of PLA ( $\rho_{PLA}$ ) and flax ( $\rho_{flax}$ ) are taken respectively as 1.24 and 1.5 gcm<sup>-3</sup> [1]. This flax  
165 density value was measured at room temperature and 50RH. The flax fibres were extracted  
166 from unidirectional preforms made for composite applications.

$$V_p = 1 - \left( \frac{1 - W_f}{\rho_{PLA}} + \frac{W_f}{\rho_{flax}} \right) \cdot \rho_c \quad (\text{Equ.4})$$

167 The assumption of an unchanged fibre density during ageing is taken. The porosity induced by  
168 manufacturing will be considered as matrix pores, and the porosity due to ageing will be  
169 referred to as defects, or specifically matrix micro-cracks or interface decohesion zones.

#### 170 2.2.5 SEM

171 Samples are observed thanks to a JEOL (Jeol, Tokyo, Japan) SEM (JSM-IT500HRSEM) at an  
172 acceleration voltage of 3 kV. For transverse section observation, sample preparation consists  
173 of embedding them into an epoxy matrix, polishing and gold-coating thanks to a sputter coater  
174 (Edward Scancoat6). For flax/PLA interface observation, samples underwent a brittle fracture  
175 under nitrogen before being sputter coated. Any surface degradation was observed, skipping  
176 the embedding step as polishing is not desirable.

#### 177 2.2.6 Biochemical analysis

178 Biochemical analysis is done on the immersion leachate to quantify the polysaccharides  
179 released by the composite. Before undergoing biochemical analysis, the leachate was  
180 centrifuged (3min at 800 rpm). Three samples of supernatants (500 $\mu$ L) were collected. First, 2-  
181 déoxy-D-ribose is added before samples are hydrolysed (2h at 120°C). Then, the uronic acid  
182 (UA) concentration was determined by an automated m-hydroxybiphenyl method [23].  
183 Additionally, the neutral sugar concentration was analysed as their alditol acetate derivatives  
184 [24] by GC gas chromatography (PerkinElmer, Clarus 580, Shelton, CT, USA) equipped with a  
185 DB 225 capillary column (J&W Scientific, Folsom, CA, USA) at 205°C, with H<sub>2</sub> as the carrier gas.

#### 186 2.2.7 AFM

187 A Multimode 8 AFM instrument (Bruker, Billerica, Massachusetts, USA) was used in PF-QNM  
188 imaging mode. This mode is based on the recording of force-distance curves at a high rate (2  
189 kHz) for a limited maximum load (200 nN here), and thus limited indentation depth (of the  
190 order of a nanometre here), while the tip scans the surface of the sample thus allowing to  
191 make topography maps. The indentation modulus is obtained from the unloading part of the  
192 force-distance curve using an appropriate contact model. We used a DMT model here, which  
193 corresponds to the Hertz contact model (small indentation depth compared to the tip apex

194 radius) modified to take into account the adhesion force (mainly due to water capillarity in our  
195 case) between the tip and the sample surface [25]. The indentation modulus obtained is  
196 similar to that obtained by nanoindentation measurements but with the required resolution to  
197 study mechanical gradients within and between cell wall layers [26]. RTESPA-525 (Bruker)  
198 silicon probe with a spherical tip apex was used here. Its spring constant (between 136 and  
199 177 N/m) was calibrated using the Sader method (<https://sadermethod.org/>), and the tip  
200 radius adjusted between 20 and 80 nm on an aramid sample having a comparable indentation  
201 modulus to flax fibre cell walls. Image resolution of 384×384 pixels was achieved, and a peak  
202 force amplitude between 50 and 100 nm was set for indentation modulus measurements. This  
203 variety of amplitude depends on the roughness of the region investigated.

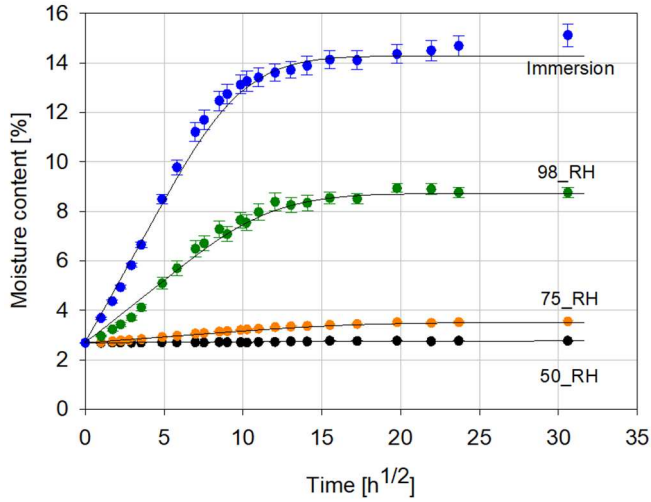
204 Only the reference, the 98\_RH and the immersion batches were investigated in regards to the  
205 mechanical properties, the density results and the SEM observation. AFM samples of 2 mm<sup>3</sup>  
206 are extracted from the middle of the centre part of the dog bones. It avoids edge influence.  
207 They are embedded into agar resin (Agar Scientific, Stansted, UK) and cut thanks to an  
208 ultramicrotome (Leica Ultracut R). Four images, including of flax fibres and PLA, were used for  
209 each reference to obtain the mean indentation modulus of the reinforcement and the matrix.  
210 The samples were analysed in a perpendicular plane of the direction with the predominant  
211 orientation of fibres (machine direction of the preform). For flax fibres, which are highly  
212 anisotropic, elliptical fibre cross-sections were not selected to avoid the risk of fibre  
213 misorientation.

## 214 **3 Results and discussion**

### 215 3.1 Moisture content evolution

216 The moisture content at saturation of the composite stored at 50% RH is  $2.6 \pm 0.1$  %. As  
217 expected for flax composite, the moisture sorption at room temperature follows Fick's law

218 [18,27] (pseudo-Fickian behaviour for immersion), as presented in Figure 1. The parameters  
 219 used for Fick's law are extracted from the experimental curves and are given in Table 2.



220

221 **Figure 2.** Moisture content evolution of a non-woven flax/PLA composite (Wf=40%) under  
 222 several ageing conditions. The dark lines correspond to Fick's laws extrapolation. The  
 223 experimental curves are used to obtain the diffusion coefficients and the moisture content at  
 224 saturation.

225

226 **Table 2.** Parameters used to calculate Fick's law, depending on the ageing condition.

	50_RH	75_RH	98_RH	Immersion
$D_{diff} \cdot 10^{-6}$ [mm <sup>2</sup> /s]	0.56	0.72	1.53	2.15
$M_{\infty}$ [%]	2.77	3.52	8.72	14.275

227

228 The moisture contents at saturation after each ageing step can be observed in Figure 2. No  
 229 clear saturation is reached in the case of immersion. Before discussing the results, note that  
 230 the stabilised moisture content of flax fibres is measured by Hill et al. [6] to be 18% at 95% RH.

231 The water uptake of virgin PLA under immersion at 25°C was measured by Deroiné et al. [28]  
232 to be  $0.59 \pm 0.03\%$ . This low moisture sorption is explained by the high glass transition  
233 temperature of PLA (60°C) [29]. As our flax/PLA composite uptakes  $15.12 \pm 0.46\%$  after 38 days  
234 ( $30 \text{ h}^{1/2}$ ) of moisture under immersion at room temperature, it can be concluded that flax  
235 fibres and/or composite microstructure (matrix pores/defects induced by ageing) are  
236 principally responsible for moisture uptake. As a consequence, PLA moisture sorption is not  
237 considered in any further detail in this work.

238 Besides a slightly higher moisture content at saturation, the moisture uptake behaviour of  
239 50\_RH and 75\_RH are similar, as observed in Table 3. The moisture uptake appears to be more  
240 critical for the 98\_RH and immersion samples. The sorption behaviour of flax fibres can explain  
241 this. It has been reported by Gouanvé et al. [8] that the mechanism of sorption of flax fibres  
242 evolves after a relative humidity close to 80%. Water molecules are absorbed on specific  
243 interaction sites or randomly adsorbed by flax, and thereafter, the water molecules cluster in  
244 the interstice and porosity of flax fibres, such as lumen or cell wall micropores [8]. Such  
245 micropores have been observed by Melelli et al. [30] on flax kink bands, where the flax  
246 structure is more heterogeneous and presents significant cavities compared to intact cell walls.  
247 This phenomenon is also observed for composites [5], where the matrix pores and the  
248 interfaces (matrix/fibres or fibres/fibres) are other places for potential water clustering.

249 Regarding the drying and restabilisation step, all batches return to a moisture content slightly  
250 higher than their initial moisture content of  $2.6 \pm 0.1\%$ , except the immersion one.

251 Interestingly, the 98\_RH samples lose more water during the drying step, meaning it has  
252 potentially a higher free/bonded water ratio than the 75\_RH and 50\_RH batches.

253

254 **Table 3.** Moisture content in non-woven flax/PLA composite (Wf=40%) at each ageing step for  
 255 all the ageing conditions. Index a, b, c highlight statistical groups determine by comparative t-  
 256 tests (p-value > 0.05 in a same group).

		50_RH	75_RH	98_RH	Immersion
Water content at saturation [-]	ageing	2.77 ± 0.01 %	3.55 ± 0.04 %	8.76 ± 0.21 %	15.12 ± 0.46 %
	drying	1.46 ± 0.04 %	1.59 ± 0.05 %	1.17 ± 0.11 %	0.24 ± 0.07 %
	restabilisation	2.72 ± 0.02 % <sup>a</sup>	2.88 ± 0.03 % <sup>b</sup>	2.86 ± 0.09 % <sup>b</sup>	1.94 ± 0.05 % <sup>c</sup>

257

258 The difference between mean water content at restabilisation is checked with t-tests. It  
 259 appears that statistically, only 75\_RH and 98\_RH have an identical mean value. In the case of  
 260 immersion, the moisture content after ageing and restabilisation is lower than the initial  
 261 moisture content.

### 262 3.2 Leaching phenomenon

263 The difference of water uptake for immersed samples is mainly due to a decrease in the  
 264 sample weight, distorting the moisture content value. Considering that the moisture content  
 265 of the immersed samples after stabilisation should be similar to other ageing conditions (ca  
 266 2.7-2.9%), this weight loss equals ca 0.8-1.0%.

267 This decrease can be induced by a leaching phenomenon already reported in the literature  
 268 [31]. It is confirmed by a change in the colour of the leachate during immersion ageing. Some  
 269 polysaccharides of the flax are dissolved and released in the surrounding water. The total mass  
 270 of samples immersed is 40 g in one litre of distilled water. Thus, considering leaching as the  
 271 only origin of the mass evolution (taken equals to 0.9%), the weight loss should induce a sugar  
 272 concentration of 360 µg/mL. However, thanks to biochemical analysis of the leachate, the total  
 273 sugar concentration only equals 25.7 µg/mL. This concentration includes 18.9 µg/mL of neutral  
 274 sugars and 6.8 µg/mL of uronic acids. The detailed biochemical analysis of the leachate is given

275 in Table 4.

276 **Table 4.** Biochemical analysis of the leachate obtained after flax/PLA non-woven composite  
277 immersion ageing. Rha = Rhamnose, Fuc= Fucose, Ara= Arabinose, Xyl= Xylose, Man=Mannose,  
278 Gal=Galactose, Glc=Glucose; U.A. = Uronic acids. N/A refers to undetected sugars.

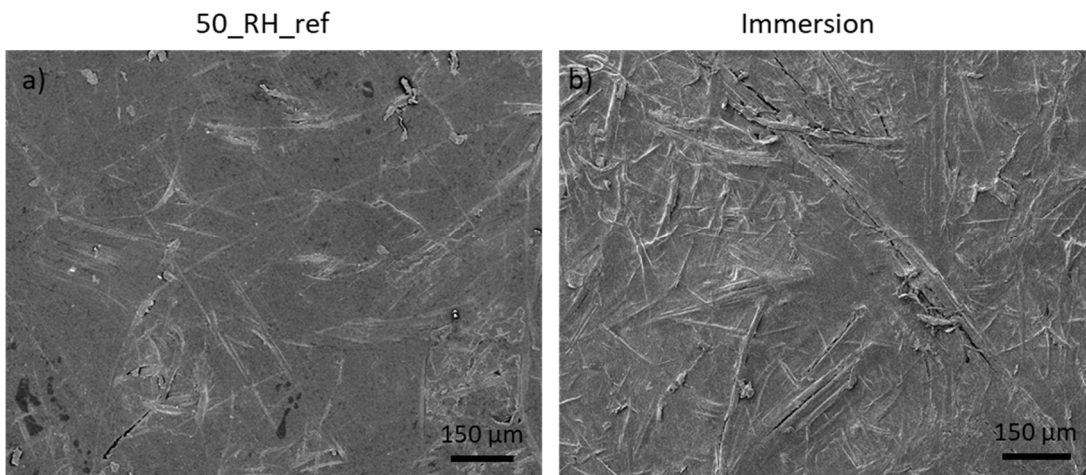
	Rha	Fuc	Ara	Xyl	Man	Gal	Glc	U.A.
Concentration [ $\mu\text{g}/\text{mL}$ ]	$4.6 \pm 1.6$	N/A	N/A	N/A	N/A	$5.2 \pm 1.7$	$9.1 \pm 4.4$	$6.8 \pm 0.3$

279

280 As dissolved polysaccharides alone cannot explain all the weight loss, PLA degradation due to  
281 fibre swelling at the surface is assumed to have a role [32]. The surface degradation is  
282 observed through SEM in Figure 3. Interestingly, the composite manufacturing process  
283 exposes flax fibres on the surface (face and edge) of unaged composites, see Figure 3. These  
284 fibres are a preferential path for water molecules, influencing the sorption kinetics observed in  
285 Figure 2.

### 286 3.3 Surface degradation

287 Additionally, an increase in degradation is observed qualitatively from the reference to  
288 immersion samples (see Figures 3.a, 3.b). Indeed, the surface roughness increases, highlighting  
289 the contribution of flax fibres swelling due to surface degradation. Additionally, cracks are  
290 reported close to the fibres, confirming PLA damaged by flax swelling.

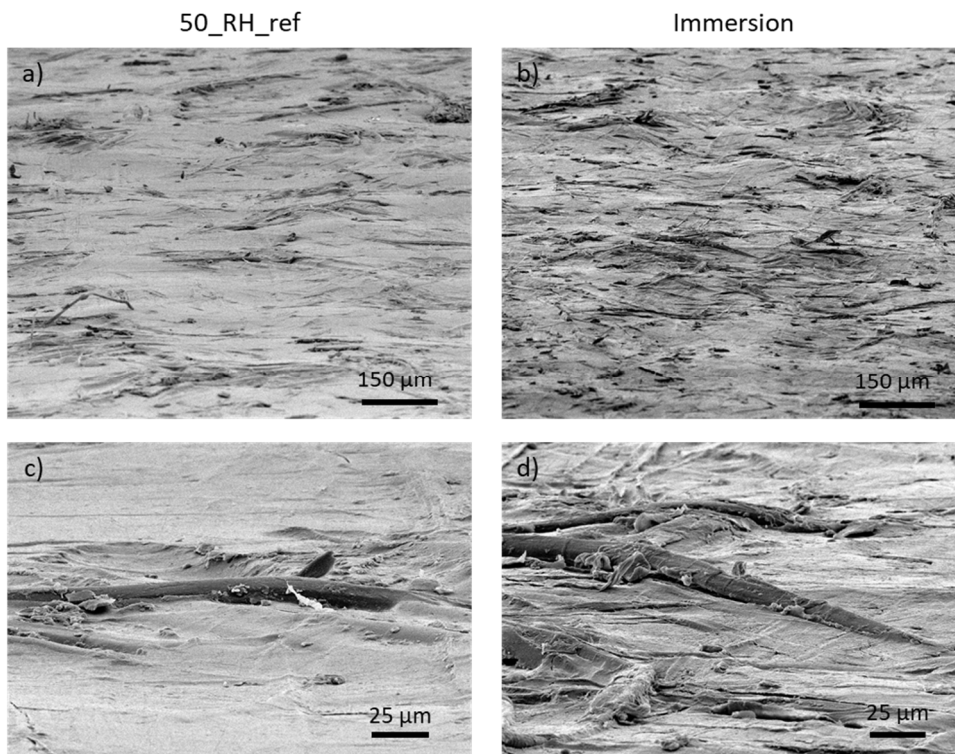


291

292 **Figure 3.** Perpendicular SEM observation of the surface degradation for 50\_RH\_ref (a) and  
 293 immersion (b) samples, focussing on the role of flax fibre swelling.

294

295 The surface degradation is more evident through tilted observation of the surfaces,  
 296 highlighting the presence of flax fibres exposed at the surface, responsible for the higher  
 297 roughness of the immersed samples. At a lower scale, as seen in Figures 4.c, 4.d, the reference  
 298 sample presents few exposed fibres at the composite face/edge, which are still surrounded by  
 299 PLA (see Figure 4.c). This is due to the manufacturing process which does not include the  
 300 presence of extra PLA layer on the edges. The number of exposed flax fibres in the immersion  
 301 samples appear higher, and they are locally detached from the PLA as gaps are present (see  
 302 Figure 4.d). They can even be uncoupled from PLA in some cases. It highlights the surface  
 303 degradation and liberation of PLA micro-particles, explaining also the weight loss.



304

305 **Figure 4.** Tilt SEM observation of surface degradation for 50\_RH\_ref (a & c) and immersion (b  
 306 & d) samples. a) & b) are global views of the surface aspect, c) & d) focus on the aspect of  
 307 exposed flax fibres.

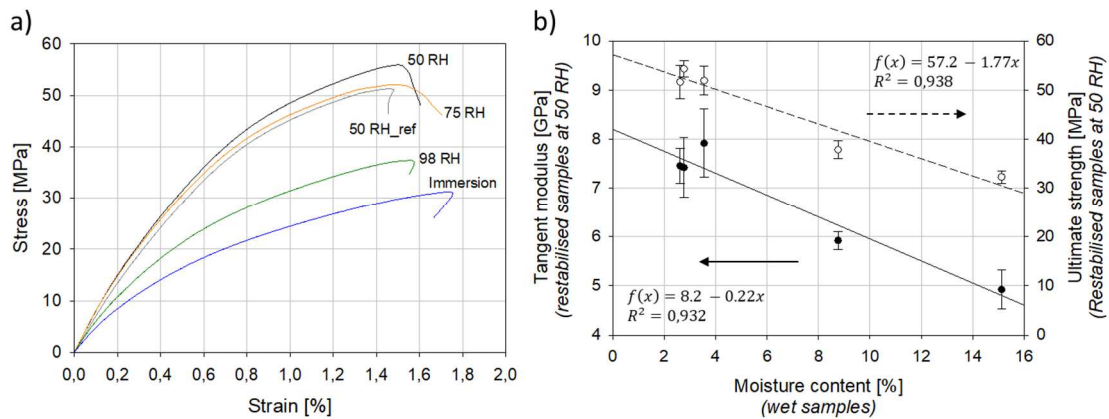
308

### 309 3.4 Tensile properties

310 By testing the mechanical properties of restabilised samples, their irreversible alteration  
 311 induced by water sorption is assessed. The tensile behaviours are represented in Figure 4.a  
 312 and the mechanical properties are summarised in Table 5. The 50\_RH and 75\_RH samples do  
 313 not present significant differences with the 50\_RH\_ref batch, as they present similar tensile  
 314 behaviour (Figure 4.a). That means the drying step (40°C until stabilisation) does not impact  
 315 the reference composite, and ageing at 75% RH does not induce irreversible change in the  
 316 flax/PLA composite. However, a decrease in stiffness and strength are observed for the 98\_RH  
 317 and immersion batches (Figure 4. b)), with a stiffness decrease of 20.3% for 98\_RH and 33.4%

318 for immersion. It agrees with the moisture uptake of wet samples, which is much higher for  
 319 98\_RH and immersion than for the three undamaged batches.

320



321

322 **Figure 5.** a) Tensile behaviour of flax/PLA composite (Wf=40%) after ageing under several  
 323 conditions, drying and restabilisation at 50% RH (restabilised state), b) Influence of moisture  
 324 content at saturation (wet state) on the tensile properties of the flax/PLA composite after  
 325 ageing, drying and restabilisation at 50% RH (restabilised state).

326

327 Interestingly, the decrease in mechanical properties of restabilised samples appears to directly  
 328 depend on the moisture content in the wet state (mainly due to the damage created by the  
 329 water uptake), as reported in Figure 4.b. These trends approach a linear correlation, with a  
 330 decrease factor of 1.77 MPa/% for strength and 0.22GPa/% for the modulus. This linearity  
 331 might be due to the progressive increase of defects inside the composite induced by the  
 332 moisture content. These linear decreases were also observed for an injected PLA/flax  
 333 immersed in seawater [33], and an increase in defects in the composite was assumed.

334 Interestingly, the strain of the composite remains around 1.6 – 1.8% (Table 5) even for 98\_RH

335 and immersed samples, which is in the same range as the failure strain of the flax fibre,  $2.1 \pm$   
336  $0.5\%$  [34]. Thus, composite behaviour is still fibre dominated even after ageing. The decrease  
337 appears similar to fibre volume reduction, indicated a loss of interface and therefore a loss of  
338 stress transfer ability from fibre.

339 It highlights the existence of a critical relative humidity between 75% RH and 98% RH (see  
340 Figure 5), where flax composites present irreversible damage. The moisture content of flax  
341 composites is described by a sigmoid [5,8] as the water starts to sorb at specific sites of  
342 interaction, then in non-specific sites before clustering micro-pores become present in flax  
343 fibres (lumen or kink-bands). A relative humidity close to 80% RH induces a drastic increase in  
344 water content in flax fibres and therefore inside the composite. This relative humidity is  
345 probably the limit to not reach to avoid irreversible damage in the composite, but its exact  
346 value may depend on the matrix mechanical behaviour. This critical relative humidity can be  
347 observed using more relative humidity ageing between 75% RH and 98% RH. Additionally, it  
348 will help to identify more precisely the nature of the trend. The dry states (lower than 2.6%)  
349 can result in different damage mechanisms, leading to another modification of mechanical  
350 properties not highlighted by the presented trend Figure 5.).

351 Interestingly, the water molecules change from the gas phase to the liquid phase when the  
352 saturation pressure of water is reached. It occurs at the physical limits of relative humidity of  
353 99.9%. For the flax/PLA non-woven composite, the moisture content jumps from 9% to 15% by  
354 switching from 98% RH to immersion ageing. Therefore, the moisture content range of 9% to  
355 15% is not reachable. However, the impact of immersion on tensile properties appears to align  
356 with vapour ageing impact, as observed in Figure 4.b. The shortcut of immersion as  
357 accelerated vapour ageing should be used carefully as the water molecules are not in the same  
358 state. Thus, ageing mechanisms could be different between vapour and immersion conditions.

359 The latter is expected to be harsher.

360

361 **Table 5.** Tensile properties of flax/PLA composite (Wf=40%) after ageing under several  
362 conditions, drying and reconditioning at 50% RH (restabilised state). The pure PLA values are  
363 extracted from a previous study [35] and measured on unaged INGEO™ PLA samples.

	50_RH_ref	50_RH	75_RH	98_RH	Immersion	Pure PLA (unaged)
Tangent modulus [GPa]	7.4 ± 0.3	7.4 ± 0.6	7.9 ± 0.7	5.9 ± 0.2	4.9 ± 0.4	3.4 ± 0.1
Ultimate strength [MPa]	51.6 ± 3.3	54.3 ± 1.6	51.9 ± 3.0	37.8 ± 1.8	32.3 ± 1.3	37.6 ± 0.8
Strain at failure [%]	1.5 ± 0.2	1.5 ± 0.1	1.4 ± 0.1	1.6 ± 0.1	1.8 ± 0.3	2.6 ± 0.4

364

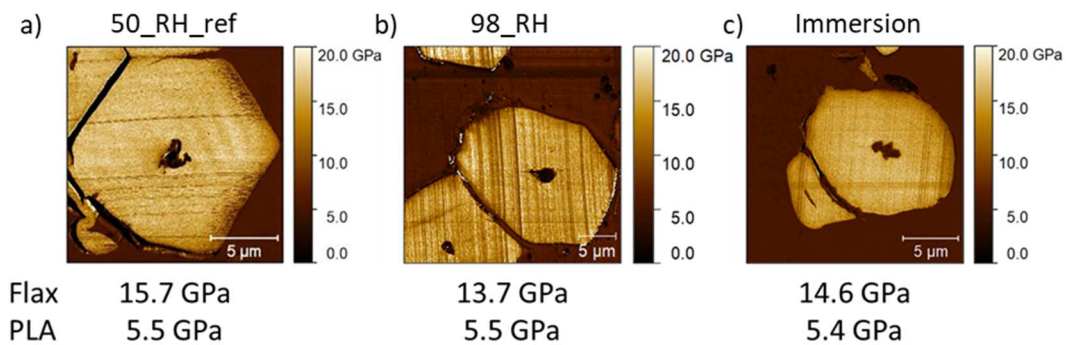
365 The amount of water uptake is the origin of composite degradation. Two hypotheses have to  
366 be verified. First, contact with water can decrease the mechanical properties of the flax fibres  
367 and the matrix. Indeed, the mechanical properties of elementary flax fibres depend on the  
368 surrounding relative humidity [23], with a decrease in strength of ca. 15% and an increase of  
369 ca. 25% of strain switching from 46% to 85% RH. Second, the composite structure can  
370 deteriorate through decohesion of the flax and matrix or by creating matrix micro-cracks  
371 induced by flax swelling and shrinkage. The combination of both phenomena will induce  
372 connected defects. For example, the decohesion at the interface creates a gap between the  
373 flax and the matrix. These gaps could be linked together by the micro-cracks present in the  
374 matrix. The reduction in composite density can be used to quantify the volume of these  
375 structural defects.

376 3.5 Evolution of flax cell wall and matrix stiffness in the composite

377 As expressed previously, one hypothesis is that ageing impacts the properties of flax and/or

378 the matrix. Therefore, their mechanical properties are assessed through AFM measurement on  
 379 the reference and the two impacted batches. Figure 5 presents the indentation modulus  
 380 mapping used for one measurement, whereas Table 6 presents the averaged indentation  
 381 modulus for flax and PLA matrix.

382



383

384 **Figure 6.** AFM indentation stiffness map for one fibre of flax/PLA composite after a) no ageing  
 385 (50\_RH\_ref), b) moisture ageing at 98% RH, c) immersion ageing with distilled water.

386

387 The evolution of constituent mechanical properties is measured at microscale level.<sup>b,b</sup> First,  
 388 the mechanical properties of PLA do not evolve during ageing, with a constant indentation  
 389 modulus value of ca. 5.5 GPa. Thus, there is no local recrystallisation of PLA. This is expected as  
 390 PLA's stiffness is relatively insensitive to immersion ageing at 25°C [28]. Indeed, Deroiné et al.  
 391 [28] reported, for virgin PLA aged six months in distilled water at 25°C, no decrease in  
 392 mechanical properties at the macro-scale and only a small chemical evolution with a decrease  
 393 of number-averaged molecular weight from 75,000 g/mol (unaged) to 66,300 g/mol.

394

395 **Table 6.** Impact of the ageing condition on the indentation stiffness of flax fibres cell walls and  
 396 PLA in the composite. It is investigated at the micro-scale level through AFM-QNM  
 397 measurements.

	50_RH_ref	98_RH	Immersion
Flax fibre indentation modulus [GPa]	15.3 ± 1.0	13.4 ± 1.8	13.9 ± 0.9
PLA indentation modulus [GPa]	5.5 ± 0.1	5.4 ± 0.3	5.4 ± 0.2

398

399 For the flax cell wall (the layer S2 of the secondary cell wall), a slight decrease appears  
 400 between the reference and the impacted samples. The impacted samples (98\_RH and  
 401 immersion) are considered statistically identical, as a t-test gives a probability of similarity  
 402 equals to 63%. However, due to the close value between the reference and the impacted  
 403 samples, their standard deviation and the operator influence on the selection of the fibres, it  
 404 can be concluded that flax cell walls present similar mechanical properties whatever the  
 405 ageing condition used. Note that these values are slightly lower than the indentation modulus  
 406 usually obtained in the literature using AFM, being between 17-22 GPa [36].

407 Interestingly, this stable indentation modulus does not agree with Le Duigou et al.'s [31]  
 408 results from nanoindentation measurements on immersed unidirectional flax/PLA composite.  
 409 Indeed, they observed a 40% decrease in nanoindentation modulus after four weeks,  
 410 compared to a 10% decrease (without considering the standard deviation) after six weeks in  
 411 this study. They explain the decrease of the mechanical properties by the solubilisation of  
 412 uronic acids, playing a role in transferring loads in the second wall (S2) of the flax fibres [31].  
 413 They observed a ratio of 2.5 between the uronic acids released and the neutral sugars. Thanks  
 414 to the biochemical analysis, this ratio is calculated to be 0.36 in our leachate, supporting the  
 415 unchanged mechanical properties of the flax fibres in the immersed samples.

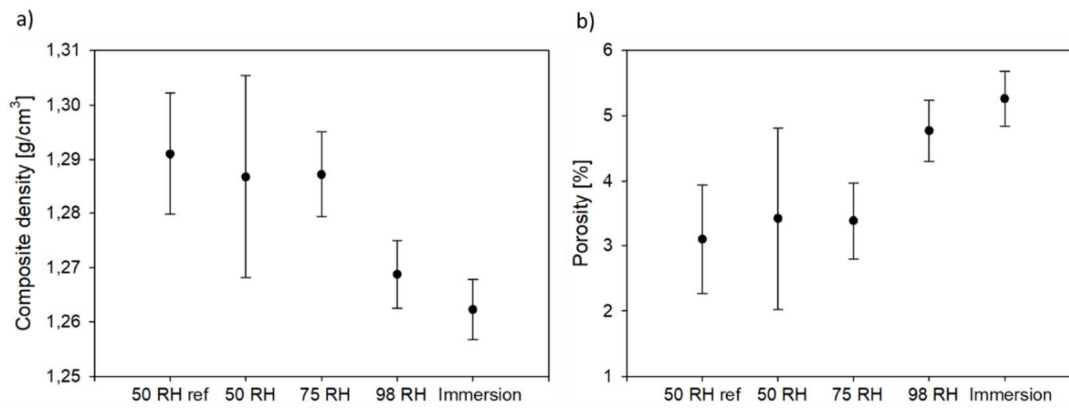
416 The difference between both experiments can be explained by the difference in flax preform  
417 and manufacturing process. Le Duigou et al. [31] used a vacuum film stacking method to  
418 manufacture flax/PLA unidirectional composite at a fibres weight fraction of 50%. This  
419 manufacturing method leads to lower compaction than the thermo-compression due to low  
420 pressure ( $\approx 0.95$  bar) [37] and potentially modify flax fibres composition as it requires the  
421 severe manufacturing condition of 180°C for 1 hour. In addition, the unidirectional orientation  
422 of fibres leads to easier leaching than random orientation as fibre percolation in the composite  
423 is higher for unidirectional. Finally, they used a magnetic stirrer, which may increase the  
424 leaching phenomenon.

425 Thus, the evolution of flax cell walls and PLA's mechanical properties cannot explain the  
426 decrease in stiffness observed at the composite scale. Therefore, the second hypothesis  
427 relating to the evolution in composite microstructure (and density) should be investigated as it  
428 may be responsible for mechanical property evolution.

### 429 3.6 Composite density evolution

430 The structural modification of the composite through ageing is potentially due to the  
431 decohesion phenomenon or micro-cracks generation in the matrix, both being related to flax  
432 fibre swelling. These mechanisms are directly linked to the composite density, as they modify  
433 its structure by damaging the interfaces for the first one and creating matrix micro-cracks for  
434 the second. The density measurement is presented in Figure 6.a). The porosity estimated is  
435 presented in Figure 6.b), considering constant flax and matrix density. However, the  
436 assumption of a constant flax density is debatable as the moisture uptake and swelling  
437 phenomena can modify flax fibre structure (not observed here by AFM), where the leaching  
438 phenomenon (immersed samples only) modifies its biochemical composition.

439



440

441 **Figure 7.** Evolution of the a) composite density and b) porosity of restabilised samples after  
 442 different ageing conditions. The porosity is calculated assuming ageing does not modify the  
 443 PLA nor flax density.

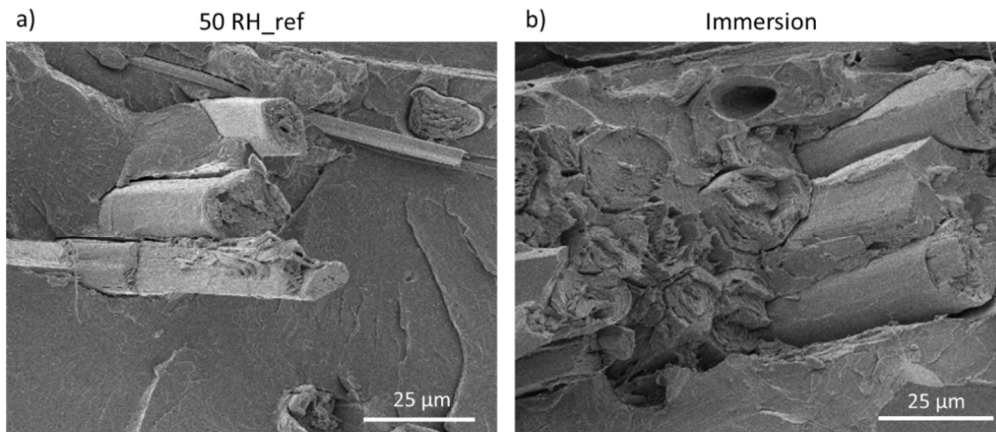
444

445 Nevertheless, the results fall in line with the mechanical properties evolution as the batches  
 446 with low density present the lowest mechanical properties. Indeed, the porosity appears to be  
 447 similar for the 50\_RH\_ref / 50\_RH / 75\_RH samples, increasing for 98\_RH and Immersion  
 448 samples (see Figure 6.b). Thus, ageing induces a modification of the inner structure of the  
 449 composite. The origin of the structural modification needs further investigations to understand  
 450 its influence on mechanical properties.

### 451 3.7 Interface decohesion

452 First, interface cohesion is checked through SEM observation on cryo-fractured samples. The  
 453 obtained pictures are presented in Figure 7, presenting flax fibres in the normal direction of  
 454 the fracture. If a damage is observed, a physical decohesion can be identified. The embedded  
 455 length should not be considered here as these samples are observed before any tensile test.

456



Cryogenic failure for interface consideration

457

458 **Figure 8.** Interface observation by SEM of flax/PLA composite after a failure of the sample  
 459 under cryogenic condition, a) observation of the reference and b) observation of the most  
 460 damaged batches, being the immersion one. No decohesion is observed after an immersion  
 461 ageing as damage is present.

462

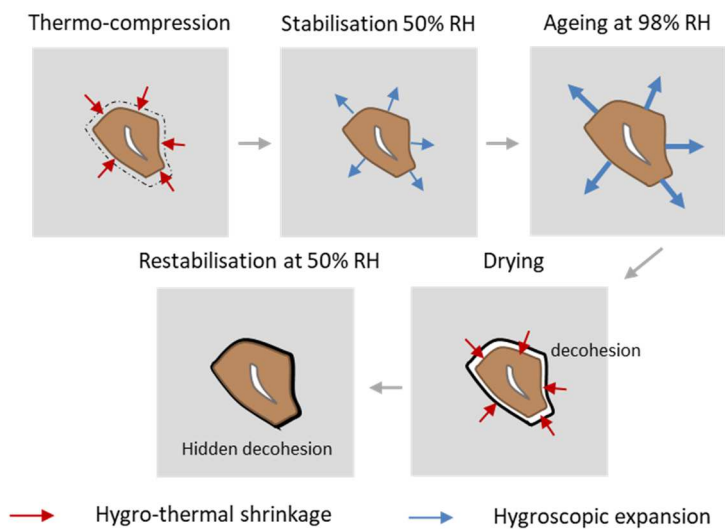
463 No significant decohesion at the flax/matrix or the flax/flax interfaces could be observed for  
 464 reference or aged flax/PLA composite. There are two explanations, the first being that the  
 465 interface is not damaged during ageing. One possibility is that fibres embedded within the PLA  
 466 in the core of the sample are not subjected to water uptake nor swelling. However, this is  
 467 unrealistic as the randomness of the preform induces interconnectivity of the flax fibres,  
 468 percolating the open edges in contact with the environment.

469 The second more realistic explanation is a damaged interface, but this could not be observed.  
 470 This damage can be due to chemical modification (leaching [31]) or hidden physical  
 471 decohesion. During the thermo-compression process, the flax fibres have a low water content  
 472 due to the high temperature. Thus, the flax fibres in the 50\_RH\_ref composite are already  
 473 constrained. In addition to the hygroscopic stress, some residual stresses due to the thermal

474 history of the polymer and flax fibres are present. In addition, flax fibres act as nucleating  
475 agents for the PLA, creating a transcrystalline layer around the fibres [38]; presence of water in  
476 the interface region, can also induce local hydrolysis of the PLA matrix.

477 During the ageing, the flax fibres swell enough to overcome the matrix's yield point locally and  
478 irreversibly deform the matrix. The drying step allows the flax fibres to retract as their water  
479 content decrease, damaging the interface and releasing the internal residual stresses. Through  
480 the restabilisation at 50% RH, the flax fibres are now free to swell, as the matrix did not  
481 constrain it, and fill the gap previously created, hiding the decohesion. This phenomenon,  
482 schematised in Figure 8, should not significantly modify the composite's density.

483



484

485 **Figure 9.** Schematic explanation of the formation of hidden decohesion due to the alternation  
486 of shrinkage and expansion of flax fibres inside the composite. Inspired from [9].

487

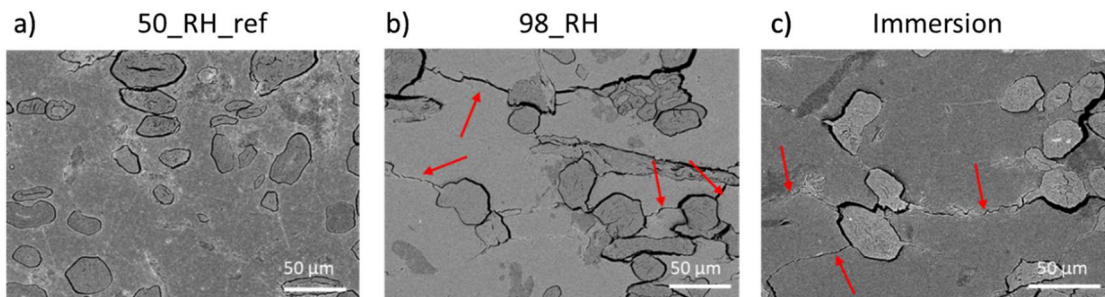
488 These potential damages at the interface can explain the decrease of the mechanical

489 properties of flax/PLA composite as the stress transfer between reinforcement and matrix.  
490 Consequently, the reinforcement of flax fibres is less efficient, inducing a decrease in the  
491 modulus and the ultimate strength of the composite without any increase in its ultimate strain.

### 492 3.8 Micro-cracks generation in the matrix

493 The swelling of the fibres during ageing has another consequence in the composite structure.  
494 As observed in Figure 10, the aged composite presents micro-cracks inside the matrix, initiated  
495 at the matrix/fibre interfaces. It suggests that the stresses applied locally by the swelled flax  
496 fibres to the matrix are higher than the ultimate strength of the matrix. Therefore, the  
497 presence of these micro-cracks decreases the mechanical properties of the composites.  
498 Indeed, they act as defects, lowering the ultimate strength of the composite but also reducing  
499 the apparent stiffness of the matrix.

500



501

502 **Figure 10.** SEM observation of flax/PLA composite after a) no ageing, b) ageing at 98% RH, c)  
503 an immersion ageing. The observations are perpendicular to the direction of the sample. The  
504 red arrows focus on the presence of matrix micro-cracks. The samples are polished.

505

506 As a first approach, the stiffness of a random non-woven composite ( $E_{NW}$ ) is estimated thanks

507 to  $E_{NW} = \frac{3}{8} \cdot E_{UD,lon gi} + \frac{5}{8} \cdot E_{UD,transv}$ , where  $E_{UD,lon gi}$  and  $E_{UD,transv}$  are the longitudinal and  
508 transversal stiffness of an equivalent unidirectional composite, respectively. The matrix  
509 stiffness is the predominant parameter of the unidirectional transversal stiffness [39]. Thus,  
510 the apparent matrix stiffness reduction due to micro-cracks directly decreases the transversal  
511 stiffness of an equivalent unidirectional composite, and so does the non-woven composite  
512 stiffness. In addition, a higher number of matrix micro-cracks might induce a lower apparent  
513 matrix stiffness. It has been observed in Figure 4.b) that the tensile stiffness of a dry sample  
514 depends on its moisture uptake in the wet state. As the number of micro-cracks should  
515 increase with higher moisture uptake (due to higher flax swelling), the generation of matrix  
516 micro-cracks is responsible for the decrease in the tensile stiffness of aged non-woven flax/PLA  
517 composites. Thus, these matrix micro-cracks decrease the composite strength but also its  
518 stiffness.

519 The fact that immersion ageing influences mechanical properties in line with vapour ageing  
520 indicates that the main damage mechanisms are mutual to immersion and vapour ageing. It  
521 can be the matrix micro-cracks or the hidden decohesion. The leaching phenomenon is  
522 discarded as it is specific to immersed samples.

523 Note that these micro-cracks were observed on epoxy embedded and polished samples (with  
524 water). The friction induced by polishing and water sorption at the surface could have been  
525 responsible for these cracks. However, the reference samples did not present micro-cracks.  
526 This gives confidence that these micro-cracks are created during ageing and not during the  
527 sample preparation. A CT-scan analysis could avoid this damaging effect and confirm the  
528 presence of the micro-cracks due to ageing. Such analysis could give additional information  
529 such as the number of matrix micro-cracks, their connectivity and their geometry.

530 Furthermore, it can confirm the link between the number of matrix micro-cracks, the water

531 uptakes at the wet state and the tensile mechanical properties of the dry sample. However,  
532 that needs a high resolution as such micro-cracks have a thickness of no more than a few  
533 micrometres.

#### 534 **4 Conclusion**

535 The evolution of the microstructure and the development of damage in a flax non-woven  
536 composite subjected to water ageing (at 50% RH / 75% RH / 98% RH / immersion) was  
537 investigated. The ageing conditions selected aimed to understand the first degradation step of  
538 a flax/PLA non-woven composite. The ageing process was monitored by following the  
539 composite's moisture content over six weeks and waiting for stabilisation in their weight  
540 before being dried and restabilised at 50% RH. Interestingly, ageing at 75% RH did not impact  
541 the mechanical properties nor the composite structure. On the other hand, samples aged at  
542 98% RH and immersion for six weeks presented a significant uptake of water, decreasing the  
543 strength and stiffness of the composites significantly.

544 A deeper analysis was conducted to better understand the ageing mechanisms. AFM  
545 investigation in peak-force mode revealed that the flax fibre cell walls and the PLA appeared to  
546 keep their initial indentation moduli. Thus, any composite softening was due to an evolution of  
547 the composite's structure, confirmed by increased porosity for the two impacted batches. The  
548 interface was observed thanks to the cryogenic failure of aged samples. No damage, including  
549 signs of decohesion of matrix and fibre, was observed. This may probably be due to the  
550 restabilisation step and the free swelling of fibres, closing ('hiding') debonding regions created  
551 by ageing. It appeared that the porosity increase was due to the creation of transverse micro-  
552 cracks induced by flax fibres swelling. That confirmed that the swelling of the fibres was  
553 responsible for the structural evolution of the composite, hidden decohesion or matrix micro-  
554 crack generation. These structural evolutions impacted the tensile properties of the flax/PLA

555 non-woven composite by decreasing its ultimate strength and stiffness.

556 On the one hand, investigating more relative humidity conditions in the range of 75RH and  
557 98RH can help identify the presence of a critical relative humidity at which mechanical  
558 properties and structure start to get significantly affected. Additionally, extending these  
559 experimental investigations of flax/PLA non-woven composites with various fibres volume  
560 fractions could lead to additional clues on the degradation mechanisms. Furthermore, using  
561 cyclic tensile loading cycles could give information on the role of interfacial defects on the  
562 composite mechanical behaviour. Finally, the effect of protecting the edges and the surface by  
563 a thin PLA layer could be scientifically interesting as it is expected to reduce the sorption  
564 kinetics, even if it is not realistic industrially speaking, unless for example using thermal  
565 methods for machining (such as laser cutting).

566

## 567 **Acknowledgements**

568 The authors want to thank the INTERREG IV Cross Channel programme for funding this work  
569 through the FLOWER project (Grant number 23).

570

## 571 **References**

- 572 [1] M. Le Gall, P. Davies, N. Martin, C. Baley, Recommended flax fibre density values for  
573 composite property predictions, *Industrial Crops and Products*. 114 (2018) 52–58.  
574 <https://doi.org/10.1016/j.indcrop.2018.01.065>.
- 575 [2] A. Lefeuvre, A. Bourmaud, C. Morvan, C. Baley, Tensile properties of elementary fibres of  
576 flax and glass: Analysis of reproducibility and scattering, *Materials Letters*. 130 (2014)  
577 289–291. <https://doi.org/10.1016/j.matlet.2014.05.115>.
- 578 [3] J. Holbery, D. Houston, Natural-fiber-reinforced polymer composites in automotive  
579 applications, *JOM*. 58 (2006) 80–86. <https://doi.org/10.1007/s11837-006-0234-2>.
- 580 [4] F. Bensadoun, B. Vanderfeesten, I. Verpoest, A.W. Van Vuure, K. Van Acker,

- 581 Environmental impact assessment of end of life options for flax-MAPP composites,  
 582 Industrial Crops and Products. 94 (2016) 327–341.  
 583 <https://doi.org/10.1016/j.indcrop.2016.09.006>.
- 584 [5] V. Gager, A. Le Duigou, A. Bourmaud, F. Pierre, K. Behloui, C. Baley, Understanding the  
 585 effect of moisture variation on the hygromechanical properties of porosity-controlled  
 586 nonwoven biocomposites, Polymer Testing. 78 (2019).  
 587 <https://doi.org/10.1016/j.polymertesting.2019.105944>.
- 588 [6] C.A.S. Hill, A. Norton, G. Newman, The water vapor sorption behavior of flax fibers—  
 589 Analysis using the parallel exponential kinetics model and determination of the  
 590 activation energies of sorption, Journal of Applied Polymer Science. 116 (2010) 2166–  
 591 2173. <https://doi.org/10.1002/app.31819>.
- 592 [7] S. Alix, E. Philippe, A. Bessadok, L. Lebrun, C. Morvan, S. Marais, Effect of chemical  
 593 treatments on water sorption and mechanical properties of flax fibres, Bioresource  
 594 Technology. 100 (2009) 4742–4749. <https://doi.org/10.1016/j.biortech.2009.04.067>.
- 595 [8] F. Gouanvé, S. Marais, A. Bessadok, D. Langevin, M. Métayer, Kinetics of water sorption  
 596 in flax and PET fibers, European Polymer Journal. 43 (2007) 586–598.  
 597 <https://doi.org/10.1016/j.eurpolymj.2006.10.023>.
- 598 [9] A. le Duigou, J. Merotte, A. Bourmaud, P. Davies, K. Belhouli, C. Baley, Hygroscopic  
 599 expansion: A key point to describe natural fibre/polymer matrix interface bond strength,  
 600 Composites Science and Technology. 151 (2017) 228–233.  
 601 <https://doi.org/10.1016/j.compscitech.2017.08.028>.
- 602 [10] A. Regazzi, S. Corn, P. Ienny, J.-C. Bénézet, A. Bergeret, Reversible and irreversible  
 603 changes in physical and mechanical properties of biocomposites during hydrothermal  
 604 aging, Industrial Crops and Products. 84 (2016) 358–365.  
 605 <https://doi.org/10.1016/j.indcrop.2016.01.052>.
- 606 [11] W.V. Srubar, C.W. Frank, S.L. Billington, Modeling the kinetics of water transport and  
 607 hydroexpansion in a lignocellulose-reinforced bacterial copolyester, Polymer. 53 (2012)  
 608 2152–2161. <https://doi.org/10.1016/j.polymer.2012.03.036>.
- 609 [12] Z. El Hachem, A. Céline, G. Challita, M.-J. Moya, S. Fréour, Hygroscopic multi-scale  
 610 behavior of polypropylene matrix reinforced with flax fibers, Industrial Crops and  
 611 Products. 140 (2019) 111634. <https://doi.org/10.1016/j.indcrop.2019.111634>.
- 612 [13] T. Joffre, E.L.G. Wernersson, A. Miettinen, C.L. Luengo Hendriks, E.K. Gamstedt, Swelling  
 613 of cellulose fibres in composite materials: Constraint effects of the surrounding matrix,  
 614 Composites Science and Technology. 74 (2013) 52–59.  
 615 <https://doi.org/10.1016/j.compscitech.2012.10.006>.
- 616 [14] M. Assarar, D. Scida, A. El Mahi, C. Poilâne, R. Ayad, Influence of water ageing on  
 617 mechanical properties and damage events of two reinforced composite materials: Flax–  
 618 fibres and glass–fibres, Materials & Design. 32 (2011) 788–795.  
 619 <https://doi.org/10.1016/j.matdes.2010.07.024>.
- 620 [15] G. Koolen, J. Soete, A.W. van Vuure, Interface modification and the influence on damage  
 621 development of flax fibre – Epoxy composites when subjected to hygroscopic cycling,  
 622 Materials Today: Proceedings. 31 (2020) S273–S279.  
 623 <https://doi.org/10.1016/j.matpr.2020.01.183>.

- 624 [16] T. Cadu, L. Van Schoors, O. Sicot, S. Moscardelli, L. Divet, S. Fontaine, Cyclic hygrothermal  
625 ageing of flax fibers' bundles and unidirectional flax/epoxy composite. Are bio-based  
626 reinforced composites so sensitive?, *Industrial Crops and Products*. 141 (2019) 111730.  
627 <https://doi.org/10.1016/j.indcrop.2019.111730>.
- 628 [17] L. Van Schoors, T. Cadu, S. Moscardelli, L. Divet, S. Fontaine, O. Sicot, Why cyclic  
629 hygrothermal ageing modifies the transverse mechanical properties of a unidirectional  
630 epoxy-flax fibres composite?, *Industrial Crops and Products*. 164 (2021) 113341.  
631 <https://doi.org/10.1016/j.indcrop.2021.113341>.
- 632 [18] A. Le Duigou, A. Bourmaud, P. Davies, C. Baley, Long term immersion in natural seawater  
633 of Flax/PLA biocomposite, *Ocean Engineering*. 90 (2014) 140–148.  
634 <https://doi.org/10.1016/j.oceaneng.2014.07.021>.
- 635 [19] A. Chilali, M. Assarar, W. Zouari, H. Kebir, R. Ayad, Effect of geometric dimensions and  
636 fibre orientation on 3D moisture diffusion in flax fibre reinforced thermoplastic and  
637 thermosetting composites, *Composites Part A: Applied Science and Manufacturing*. 95  
638 (2017) 75–86. <https://doi.org/10.1016/j.compositesa.2016.12.020>.
- 639 [20] N. Martin, P. Davies, C. Baley, Evaluation of the potential of three non-woven flax fiber  
640 reinforcements: Spunlaced, needlepunched and paper process mats, *Industrial Crops and  
641 Products*. 83 (2016) 194–205. <https://doi.org/10.1016/j.indcrop.2015.10.008>.
- 642 [21] D. Pantaloni, D. Shah, C. Baley, A. Bourmaud, Monitoring of mechanical performances of  
643 flax non-woven biocomposites during a home compost degradation, *Polymer  
644 Degradation and Stability*. 177 (2020) 109166.  
645 <https://doi.org/10.1016/j.polymdegradstab.2020.109166>.
- 646 [22] C. Baley, A. Le Duigou, A. Bourmaud, P. Davies, Influence of drying on the mechanical  
647 behaviour of flax fibres and their unidirectional composites, *Composites Part A: Applied  
648 Science and Manufacturing*. 43 (2012) 1226–1233.  
649 <https://doi.org/10.1016/j.compositesa.2012.03.005>.
- 650 [23] A. Thuault, S. Eve, D. Blond, J. Bréard, M. Gomina, Effects of the hygrothermal  
651 environment on the mechanical properties of flax fibres, *Journal of Composite Materials*.  
652 48 (2014) 1699–1707. <https://doi.org/10.1177/0021998313490217>.
- 653 [24] A.B. Blakeney, P.J. Harris, R.J. Henry, B.A. Stone, A simple and rapid preparation of alditol  
654 acetates for monosaccharide analysis, *Carbohydrate Research*. 113 (1983) 291–299.  
655 [https://doi.org/10.1016/0008-6215\(83\)88244-5](https://doi.org/10.1016/0008-6215(83)88244-5).
- 656 [25] K.L. Johnson, J.A. Greenwood, An Adhesion Map for the Contact of Elastic Spheres,  
657 *Journal of Colloid and Interface Science*. 192 (1997) 326–333.  
658 <https://doi.org/10.1006/jcis.1997.4984>.
- 659 [26] A. Melelli, O. Arnould, J. Beaugrand, A. Bourmaud, The Middle Lamella of Plant Fibers  
660 Used as Composite Reinforcement: Investigation by Atomic Force Microscopy,  
661 *Molecules*. 25 (2020) 632. <https://doi.org/10.3390/molecules25030632>.
- 662 [27] W. Wang, M. Sain, P.A. Cooper, Study of moisture absorption in natural fiber plastic  
663 composites, *Composites Science and Technology*. 66 (2006) 379–386.  
664 <https://doi.org/10.1016/j.compscitech.2005.07.027>.
- 665 [28] M. Deroiné, A. Le Duigou, Y.-M. Corre, P.-Y. Le Gac, P. Davies, G. César, S. Bruzard,  
666 Accelerated ageing of polylactide in aqueous environments: Comparative study between

- 667 distilled water and seawater, *Polymer Degradation and Stability*. 108 (2014) 319–329.  
 668 <https://doi.org/10.1016/j.polymdegradstab.2014.01.020>.
- 669 [29] G. Francois, B. Stéphane, D. Guillaume, F. Pascale, C. Emmanuelle, G. Jeff, G. Régis, G.  
 670 Matthieu, H. Arnaud, L. Fabienne, others, Pollution des océans par les plastiques et les  
 671 microplastiques Pollution of oceans by plastics and microplastics, *Techniques de*  
 672 *l'Ingenieur*. (2020) BIO9300. <https://archimer.ifremer.fr/doc/00663/77471/>.
- 673 [30] A. Melelli, S. Durand, O. Arnould, E. Richely, S. Guessasma, F. Jamme, J. Beaugrand, A.  
 674 Bourmaud, Extensive investigation of the ultrastructure of kink-bands in flax fibres,  
 675 *Industrial Crops and Products*. 164 (2021) 113368.  
 676 <https://doi.org/10.1016/j.indcrop.2021.113368>.
- 677 [31] A. Le Duigou, A. Bourmaud, C. Baley, In-situ evaluation of flax fibre degradation during  
 678 water ageing, *Industrial Crops and Products*. 70 (2015) 204–210.  
 679 <https://doi.org/10.1016/j.indcrop.2015.03.049>.
- 680 [32] T. Bayerl, M. Geith, A.A. Somashekar, D. Bhattacharyya, Influence of fibre architecture on  
 681 the biodegradability of FLAX/PLA composites, *International Biodeterioration &*  
 682 *Biodegradation*. 96 (2014) 18–25. <https://doi.org/10.1016/j.ibiod.2014.08.005>.
- 683 [33] A. Le Duigou, P. Davies, C. Baley, Seawater ageing of flax/poly(lactic acid) biocomposites,  
 684 *Polymer Degradation and Stability*. 94 (2009) 1151–1162.  
 685 <https://doi.org/10.1016/j.polymdegradstab.2009.03.025>.
- 686 [34] C. Baley, A. Bourmaud, Average tensile properties of French elementary flax fibers,  
 687 *Materials Letters*. 122 (2014) 159–161. <https://doi.org/10.1016/j.matlet.2014.02.030>.
- 688 [35] D. Pantaloni, L. Ollier, D.U. Shah, C. Baley, E. Rondet, A. Bourmaud, Can we predict the  
 689 microstructure of a non-woven flax/PLA composite through assessment of anisotropy in  
 690 tensile properties?, *Composites Science and Technology*. 218 (2022) 109173.  
 691 <https://doi.org/10.1016/j.compscitech.2021.109173>.
- 692 [36] O. Arnould, D. Siniscalco, A. Bourmaud, A. Le Duigou, C. Baley, Better insight into the  
 693 nano-mechanical properties of flax fibre cell walls, *Industrial Crops and Products*. 97  
 694 (2017) 224–228. <https://doi.org/10.1016/j.indcrop.2016.12.020>.
- 695 [37] V. Popineau, A. Céline, M. Le Gall, L. Martineau, C. Baley, A. Le Duigou, Vacuum-Bag-Only  
 696 (VBO) Molding of Flax Fiber-reinforced Thermoplastic Composites for Naval Shipyards,  
 697 *Appl Compos Mater*. (2021). <https://doi.org/10.1007/s10443-021-09890-2>.
- 698 [38] S. Garkhail, B. Wieland, J. George, N. Soykeabkaew, T. Peijs, Transcrystallisation in PP/flax  
 699 composites and its effect on interfacial and mechanical properties, *J Mater Sci*. 44 (2009)  
 700 510–519. <https://doi.org/10.1007/s10853-008-3089-9>.
- 701 [39] I.M. Daniel, O. Ishai, *Engineering mechanics of composite materials*, 2nd ed, Oxford  
 702 University Press, New York, 2006.  
 703

## 704 **Figures captions**

705 **Figure 1.** Schematic representation of the ageing protocol applied to a flax/PLA non-woven

706 composite with a fibre volume fraction of 36%.

707 **Figure 2.** Moisture content evolution of a non-woven flax/PLA composite (Wf=40%) under  
708 several ageing conditions. The dark lines correspond to Fick's laws extrapolation. The  
709 experimental curves are used to obtain the diffusion coefficients and the moisture content at  
710 saturation.

711 **Figure 3.** Perpendicular SEM observation of the surface degradation for 50\_RH\_ref (a) and  
712 immersion (b) samples, focussing on the role of flax fibre swelling.

713 **Figure 4.** Tilt SEM observation of surface degradation for 50\_RH\_ref (a&c) and immersion  
714 (b&d) samples. a) & b) are global views of the surface aspect, c) & d) focus on the aspect of  
715 exposed flax fibres.

716 **Figure 5.** a) Tensile behaviour of flax/PLA composite (Wf=40%) after ageing under several  
717 conditions, drying and restabilisation at 50% RH (restabilised state), b) Influence of moisture  
718 content at saturation (wet state) on the tensile properties of the flax/PLA composite after  
719 ageing, drying and restabilisation at 50% RH (restabilised state).

720 **Figure 6.** AFM indentation stiffness map for one fibre of flax/PLA composite after a) no ageing  
721 (50\_RH\_ref), b) moisture ageing at 98% RH, c) immersion ageing with distilled water.

722 **Figure 7.** Evolution of the a) composite density and b) porosity of restabilised samples after  
723 different ageing conditions. The porosity is calculated assuming ageing does not modify the  
724 PLA nor flax density.

725 **Figure 8.** Interface observation by SEM of flax/PLA composite after a failure of the sample  
726 under cryogenic condition, a) observation of the reference and b) observation of the most  
727 damaged batches, being the immersion one. No decohesion is observed after an immersion

728 ageing as damage is present.

729 **Figure 9.** Schematic explanation of the formation of hidden decohesion due to the alternation  
730 of shrinkage and expansion of flax fibres inside the composite. Inspired from [9].

731 **Figure 10.** SEM observation of flax/PLA composite after a) no ageing, b) ageing at 98% RH, c)  
732 an immersion ageing. The observations are perpendicular to the direction of the sample. The  
733 red arrows focus on the presence of matrix micro-cracks. The samples are polished.

734

### 735 **Tables Captions**

736 **Table 1.** Salt used for conditioning the chambers and the exact relative humidity condition  
737 induced by them.

738 **Table 2.** Parameters used to calculate Fick's law, depending on the ageing condition.

739 **Table 3.** Moisture content in non-woven flax/PLA composite (Wf=40%) at each ageing step for  
740 all the ageing conditions.

741 **Table 4.** Biochemical analysis of the leachate obtained after flax/PLA non-woven composite  
742 immersion ageing. Rha = Rhamnose, Fuc= Fucose, Ara= Arabinose, Xyl= Xylose, Man=Mannose,  
743 Gal=Galactose, Glc=Glucose; U.A. = Uronic acids. N/A refers to undetected sugars.

744 **Table 5.** Tensile properties of flax/PLA composite (Wf=40%) after ageing under several  
745 conditions, drying and reconditioning at 50% RH (restabilised state). The pure PLA values are  
746 extracted from a previous study [35] and measured on unaged INGEO™ PLA samples.

747 **Table 6.** Impact of the ageing condition on the indentation stiffness of flax fibres cell walls and  
748 PLA in the composite. It is investigated at the micro-scale level through AFM-QNM

749 measurements.